Latin American Journal of Solids and Structures
www.lajss.org

Ultimate Strength of Continuous Stiffened Aluminium Plates Under Combined Biaxial Compression and Lateral Pressure

Abstract

Ultimate compressive strength of welded stiffened aluminium plates under combined biaxial in-plane compression and different levels of lateral pressure is assessed herein. A numerical database of the ultimate strengths for stiffened aluminium plates is generated at first. Then, regression analysis is applied in order to derive the empirical formulations as functions of two parameters, namely the plate slenderness ratio and the column (stiffener) slenderness ratio. The formulae implicitly include the effects of initial imperfections and heat affected zone.

Keywords

Ultimate strength; Continuous stiffened aluminium plates; Biaxial compression; Lateral pressure; Empirical formulation; Heat-affected zone; Finite Element Method (FEM); Regression analysis.

Mohammad Reza Khedmati [*] [a]
Hamid Reza Memarian [a]
Manouchehr Fadavie [a]
Mohammad Reza Zareei [b]

[a] Department of Marine Technology, Amirkabir University of Technology, 424 Hafez Avenue, Tehran 15916-34311, Iran
[b] Shipbuilding Group, Faculty of Engineering, Chabahar Maritime University, Chabahar 99717-56499, Iran

[*] Author e-mail: khedmati@aut.ac.ir

http://dx.doi.org/10.1590/1679-78251516

Received 17.08.2014
In Revised Form 21.10.2014
Accepted 23.10.2014
Available online 11.11.2014

NOMENCLATURE

a	Length of local plate panels
a_1 *to* a_2	Constant powers
b	Breadth of local plate panels
c	Coefficient to define the maximum magnitude of the initial deflection
c_1 *to* c_3	Constant coefficients
d_1 *to* d_3	Constant coefficients
E	Young's modulus

b_f	Flange breadth of longitudinal stiffener
h	Water head (pressure)
h_w	Web height of longitudinal stiffener
I	Moment of inertia of a stiffener with its attached plating
m_1 *to* m_6	Constant coefficients
n_1 *to* n_6	Constant coefficients
$r\ (=\sqrt{\frac{I}{A}}\ )$	Radius gyration of a stiffener with its attached plating
$t\ (=t_p)$	Plate thickness
t_f	Flange thickness of longitudinal stiffener
t_w	Web thickness of longitudinal stiffener
u	Displacement along x-axis
v	Displacement along y-axis
w	Displacement along z-axis
$W_{0\max}$	Maximum magnitude of initial deflection
$\beta\ (=\frac{b}{t}\sqrt{\frac{\sigma_Y}{E}}\ )$	Slenderness parameter of the plate
$\lambda\ (=\frac{a}{\pi.r}\sqrt{\frac{\sigma_Y}{E}})$	Column slenderness parameter of the stiffened plate
ν	Poisson's ratio
σ_x	Average longitudinal strength at the ultimate limit state
σ_y	Average transverse strength at the ultimate limit state
σ_{uxq}	Ultimate strength under combined longitudinal compression and lateral pressure obtainable from Khedmati *et al.* (2010)
σ_{uyq}	Ultimate strength under combined transverse compression and lateral pressure obtainable from Khedmati *et al.* (2014*b*)
σ_Y	Yield stress
θ_x	Rotation about x-axis
θ_y	Rotation about y-axis
θ_z	Rotation about z-axis

1 INTRODUCTION

Structural design of marine structures can be performed using either traditional allowable stress design (ASD) or limit state design (LSD). A great attention has been paid in recent years towards extending the wide range of applications of limit state design to some remaining marine structures, especially merchant ships.

Although large merchant ships are usually built in steel, aluminium alloys may be employed in construction of small-to-moderate size merchant ships. Owing to the differences that exist between the behaviour of steels and that of aluminium alloys, available formulations for steel structures cannot be directly applied to the aluminium structures, even with considering suitable conversion coefficients. That is why, there is a need to develop limit state equations specific to structures made in aluminium alloys.

Stiffened aluminium plates as the main supporting elements in the structure of high-speed ships and also in the superstructures of the ships, are primarily required to resist against in-plane compressive forces acting along their length and/or breadth. Moreover, lateral pressure loading may also be present beside the in-plane loads. Ultimate limit state (ULS) is the main limit state governing the collapse of stiffened plates. The stiffened plates may experience different types of buckling failures when subjected to above-mentioned loads.

The ultimate strength of stiffened aluminium AA6082-T6 plates under the axial compression was investigated by Aalberg *et al.* (1998) using numerical and experimental methods. Hopperstad *et al.* (1998) carried out a study with the objective of assessing the reliability of non-linear finite element analyses in predictions on ultimate strength of aluminium plates subjected to in-plane compression. Some initial experimental and numerical simulations on the torsional buckling of flatbars in aluminium plates have been also performed by Zha *et al.* (2001) and also Zha and Moan (2003). A numerical benchmark study to present reliable finite element models to investigate the behaviour of axially compressed stiffened aluminium plates (including extruded profiles) was performed by Rigo *et al.* (2003).

Paik *et al.* (2005) presented a methodology for ultimate limit state design of multi-hull ships made in aluminium. The impact of initial imperfections due to the fusion welding on the ultimate strength of stiffened aluminium plates was studied by Paik *et al.* (2006) [8]. Paik (2007) derived empirical formulations for predicting the ultimate compressive strength of welded aluminium stiffened plates. Mechanical collapse tests on stiffened aluminium structures for marine applications were performed by Paik *et al.* (2008). Khedmati *et al.* (2009) performed a thorough sensitivity analysis on the elastic buckling and ultimate strength of continuous stiffened aluminium plates under combined longitudinal in-plane compression and lateral pressure. Also, in another study, Khedmati *et al.* (2010*a*) investigated the post-buckling behaviour and strength of multi-stiffened aluminium plates under combined longitudinal in-plane compression and lateral pressure. Later, empirical formulations for estimation of ultimate strength of continuous stiffened aluminium plates under combined longitudinal in-plane compression and lateral pressure were derived by Khedmati *et al.* (2010*b*). Also, Khedmati *et al.* (2014*b*) extended their empirical formulations to the case of continuous stiffened aluminium plates under combined transverse in-plane compression and lateral pressure

This paper is a continuation of the studies made by Khedmati *et al.* (2010*b*, 2014*b*), in order to further develop empirical formulations for prediction of ultimate strength of continuous stiffened aluminium plates under combined biaxial in-plane compression and lateral pressure. The ultimate compressive strength data numerically obtained by the authors is used for deriving the formulations which are expressed as functions of two parameters, namely the plate slenderness ratio and the column (stiffener) slenderness ratio. Regression analysis is used in order to derive the empirical formulations. The formulae implicitly include the effects of weld induced initial imperfections and softening in the heat affected zone.

2 ELASTIC_PLASTIC LARGE DEFLECTION ANALYSIS

A number of stiffened aluminium plate models are created in order to be analysed using finite element method.

2.1 Geometrical Characteristics of the Models

Three types of models are considered. Geometrical characteristics of all stiffened plate models are given in Table 1. In each type, three different shapes of stiffeners (Flat, Angle and Tee) have been attached to the isotropic plate, Figure 1. The stiffened plates of each type have the same moment of inertia. Types 1, 2 and 3 correspond respectively to weak, medium and heavy stiffeners.

Type	Model	Shape	Plate			Longitudinal stiffener				Stiffened Plate		
			a	b	t	t_w	h_w	t_f	b_f	I	β	λ
			mm	mm	mm	mm	mm	mm	mm	mm^4	-	-
1: Weak stiffener	F1	Flat	900	300	7	5	53.5	---	---	226254	2.603	0.787
	L1	Angle			6	4	40	4	20	226380	3.037	0.790
	T1	Tee			6	4	40	4	20	226380	3.037	0.790
2: Medium stiffener	F2	Flat	900	300	7	6	82.2	---	---	804521	2.603	0.426
	L2	Angle			6	5	60	5	30	803652	3.037	0.411
	T2	Tee			6	5	60	5	30	803652	3.037	0.411
3: Heavy stiffener	F3	Flat	900	300	8	10	107.6	---	---	2503753	2.278	0.273
	L3	Angle			6	8	80	8	40	2505550	3.037	0.271
	T3	Tee			6	8	80	8	40	2505550	3.037	0.271

Table 1: Geometrical characteristics of the stiffened aluminium plate models.

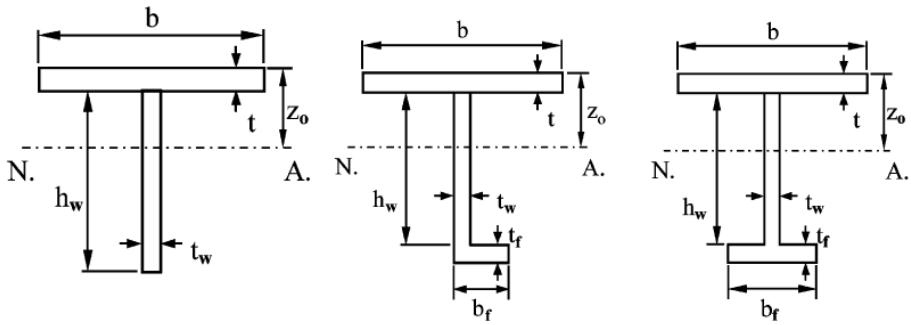
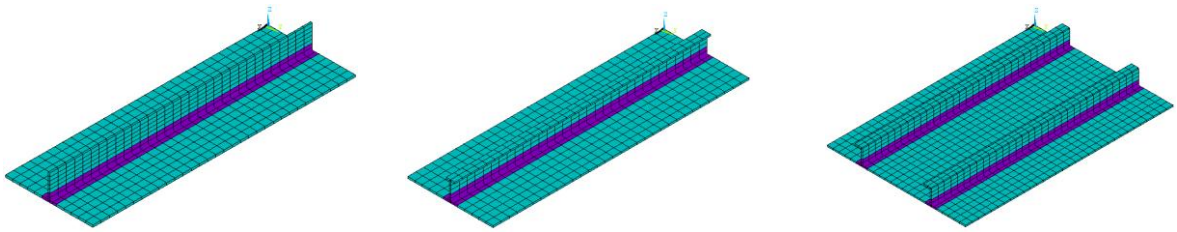


Figure 1: Cross-sectional geometries of stiffened aluminium plates (Paik *et al.* 2008).

2.2 Finite Element Code and Details of Descretisations

ANSYS FEM program (2003) is utilised in order to perform elastic-plastic large deflection analyses on the stiffened aluminium plate models. Both material and geometric nonlinearities are taken into account. The four-node SHELL43 elements are used for discretisation of the stiffened plate models. The SHELL43 element has six degrees of freedom at each node: translations in the nodal x, y, and z directions and rotations about the nodal x, y, and z axes.



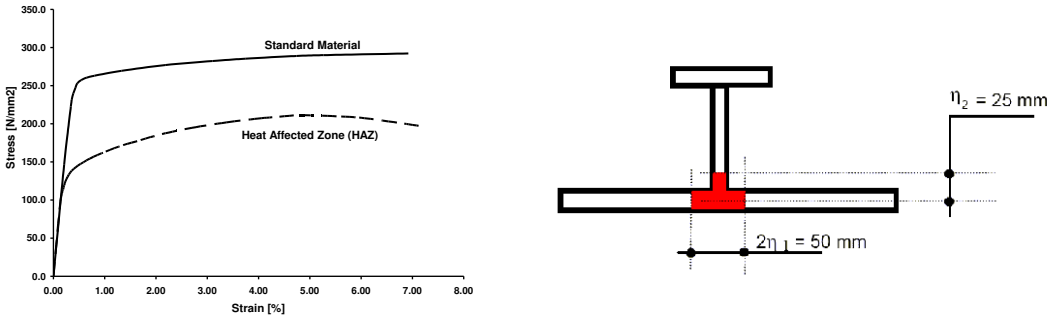
(a) Flat bar stiffened plate (b) Tee bar stiffened plate (c) Angle bar stiffened plate

Figure 2: Typical examples of the discretised stiffened plate models.

Based on the experience gained by Khedmati *et al.* (2009, 2010*b*), 300 elements are used to descretise each local plate panel (the panel surrounded by successive longitudinal or transverse stiffeners), 6 to 7 and 5 to 6 elements are also considered respectively along web and flange stiffener. Figure 2 shows typical examples of the stiffener mesh models.

2.3 Mechanical Behaviour of Material

The Young modulus and the Poisson's ratio of the aluminium alloy material are 70.475 GPa and 0.3 respectively. The stress-strain relationship of the aluminium alloy is shown in Figure 3 (a). The breadth of heat affected zone (HAZ) is assumed to be 50 mm in the plate and 25 mm in the stiffener web, at the plate-stiffener junction, Figure 3(b).



(a) Stress-strain behaviour (b) Extent of the heat affected zone (HAZ)

Figure 3: Stress-strain behaviour of the material and extent of the HAZ.

2.4 Extent of the Model, Boundary Conditions and Loading Sequence

In most of the studies regarding the buckling and ultimate strength of plates, an isolated plate surrounded between longitudinal stiffeners and transverse frames is considered assuming simply-supported boundaries around the plate. However, in continuous plating subjected to a high lateral pressure, the plate deflects in the same direction in all adjacent spans or bays. Therefore, for large lateral pressure the plate can be considered as clamped along its edges. As a result, according to the numerical studies on continuous ship bottom plating under combined in-plane compression and lateral pressure (Yao *et al.* 1998), both elastic buckling strength and ultimate strength become larger than those for the simply-supported isolated plates. Thus, continuous stiffened plate models are to be used in such analyses (Yao *et al.* 1998).

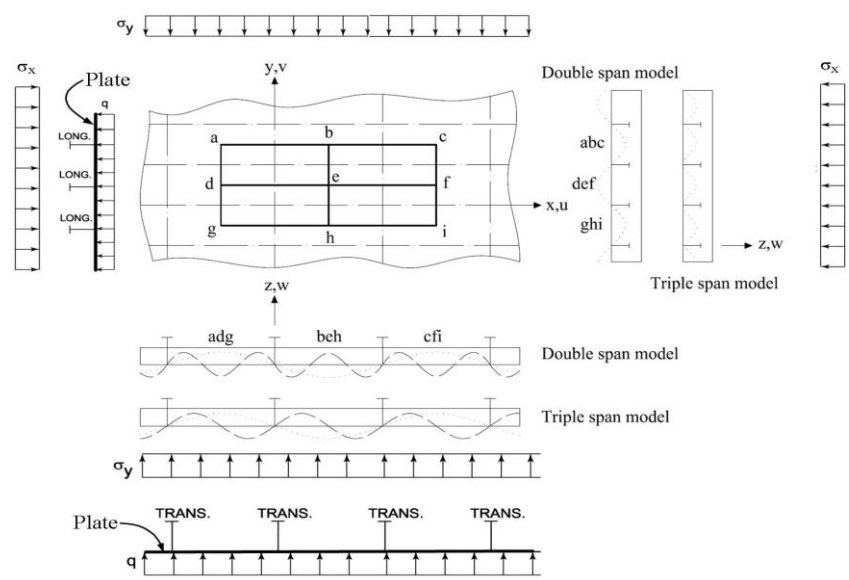


Figure 4: Extent of the continuous stiffened plate models for analysis in which q is the lateral pressure acting perpendicularly on the plate region (Yao *et al.* 1998).

A double span- double bay (DS-DB) model (region *abde* in Figure 4) has been chosen for the analysis of stiffened aluminium plates with symmetrical stiffeners (Memarian 2011). For the analysis of the stiffened plates with non-symmetrical stiffeners, a double span-triple bay (DS-TB) model (region *abgh* in Figure 4) has been considered (Memarian 2011). The boundary conditions of the analysed models are as follow:

- Periodically continuous conditions (equality of displacement along x-axis, displacement along z-axis, rotation about x-axis, rotation about y-axis and rotation about z-axis) are imposed at the same x-coordinate along the longitudinal edges in the triple bay models (i.e. along *ab* and *gh*). These conditions are defined as below:

$$\begin{aligned} u_{ab} &= u_{gh} \\ w_{ab} &= w_{gh} \\ \theta_{x-ab} &= \theta_{x-gh} \\ \theta_{y-ab} &= \theta_{y-gh} \\ \theta_{z-ab} &= \theta_{z-gh} \end{aligned} \tag{1}$$

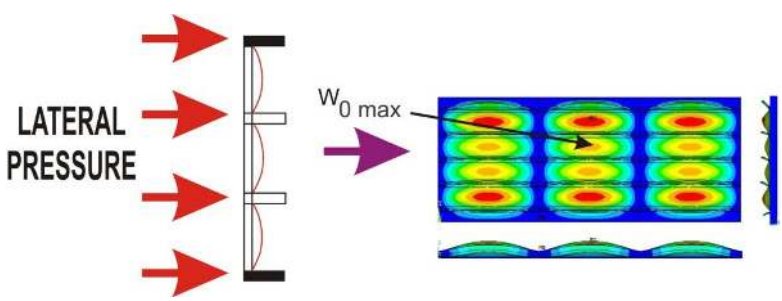
- Symmetry conditions are imposed at the same x-coordinate along the longitudinal edges in the double bay models (i.e. along *ab* and *de*).

- Symmetry conditions are imposed at the same y-coordinate along the transverse edges in the double span models (i.e. along *adg* and *beh*).

- Although transverse frames are not modelled, the out-of-plane deformation of plate is restrained along its junction line with the transverse frame.

- To consider the plate continuity, in-plane movement of the plate edges in their perpendicular directions is assumed to be uniform.

After producing initial deflection in the stiffened plate models, lateral pressure is applied first on it until the assumed levels. Then, biaxial in-plane compression with different combinations of longitudinal/transverse stresses is exerted on the stiffened plate model.



(a) Pressure loading of stiffened plate models.

Trans.

1	1.05	Long.
1.05	1	
1	1.05	Long.
1.05	1	

(a) Coefficients for correction of maximum initial deflection in the plate panels

Figure 5: Procedure to generate initial deflection.

2.5 Initial Imperfections

In order to simulate the complex pattern of initial deflection (Yao *et al.* 1998), lateral pressure is applied first on the stiffened plate model and a linear elastic finite element analysis is carried out. Such an analysis is repeated in a trial and error sequence of calculations until the deflection of plate reaches to the average value given by equation (2).

$$W_{0\max} = c\beta^2 t \tag{2}$$

The value of coefficient c depends on the level of initial deflection. Smith *et al.* (1987) proposed the maximum magnitude of initial deflection, $W_{0\max}$ as follows:

.

$$W_{0\max} = \begin{cases} 0.025\beta^2 t & \text{for slight level} \\ 0.1\beta^2 t & \text{for average level} \\ 0.3\beta^2 t & \text{for severe level} \end{cases} \tag{3}$$

The relationships given in the equations (2) and (3) are usually employed for strength assessment of steel structures. However, they can also be generalised to the case of aluminium structures, provided that a suitable amount of the coefficient c is adopted. Based on the earlier studies made by Paik *et al.* (2008) and also those of Khedmati *et al.* (2010b) and Memarian (2011), the coefficient c is assumed to be of the value of 0.05 reflecting the average value of initial deflection in ship plating evaluated by Varghese (1998). Thus, the final value of the maximum plate deflection is adopted as:

$$W_{0\max} = 0.05\beta^2 t \tag{4}$$

After satisfying this condition, the data information *i.e* the coordinates of nodal points, element coordinates and boundary conditions, are extracted and transferred to a new finite element mesh. The new model is used for a non-linear FEA analysis of the stiffened plate subjected to biaxial in-plane compression combined with variable levels of the lateral pressure. The procedure of generating initial deflection is shown schematically in Figure 5 (a). After this step, lateral pressure is first applied until the assumed levels, before the application of in plane biaxial compression load (Memarian 2011, Khedmati 2000).

The values of maximum initial deflections in the adjacent local plate panels in the analysed models are corrected with some experience-based coefficients as defined in the Figure 5 (b) (Khedmati 2000), in order to overcome divergence problems.

In addition to the initial deflections in the plate panels and successively in the attached stiffeners, material softening in the heat affected zones (HAZ) is taken into account.

2.6 Arc-length Method

The arc-length method is activated herein to help avoid bifurcation points and track unloading. This method causes the equilibrium iterations to converge along an arc, thereby often preventing divergence, even when the slope of the load versus deflection curve becomes zero or negative.

Reference	Model	Ultimate Load [kN]		
		In reference (experiment)	In reference (ABAQUS)	In present study (ANSYS)
Zha and Moan (2003)	A7 (material: AA5083–H116)	456.82	435.53	479.94
	A16 (material: AA6082-T6)	737.12	738.22	761.47

Table 2: Comparison of the ultimate strengths for the stiffened aluminium plates.

2.7 Validation of Numerical Model

As it was already stated, the current study is a continuation of the work reported in Khedmati *et al.* (2010*b*, 2014*b*). Thus, its results are fully supported by the numerous validation analyses already performed by Khedmati *et al.* (2009). An extract of the validation analyses made by Khedmati *et al.* (2009) is described in the Table 2. It can be easily confirmed that the results obtained in this study are in good agreement with the results available in the literature.

2.8 Demonstration of the Results

The full-range curves of σ_y (nondimensionalised by σ_{uyq}) versus σ_x (nondimensionalised by σ_{uxq}) are traced for various ratios of σ_y / σ_x in the current study. Three values of 0.30, 0.45 and 0.60 are assumed for the ratio of σ_y / σ_x. It should be emphasised that all of the models represented in Table 1 have been already analysed by Khedmati *et al.* (2009, 2014*a*) under combined longitudinal compression and lateral pressure or under combined transverse compression and lateral pressure, respectively. The results of the calculations are drawn in a σ_y / σ_{uyq} - σ_x / σ_{uxq} coordinate system as shown in Figure 6. The two points with the coordinates of (1.0, 0.0) and (0.0, 1.0) shown with solid circles in the Figure 6 represent the states of combined longitudinal compression and lateral pressure or combined transverse compression and lateral pressure, respectively. The next step will be drawing the envelope curve or the so-called "*Interaction Diagram*" in the Figure 6.

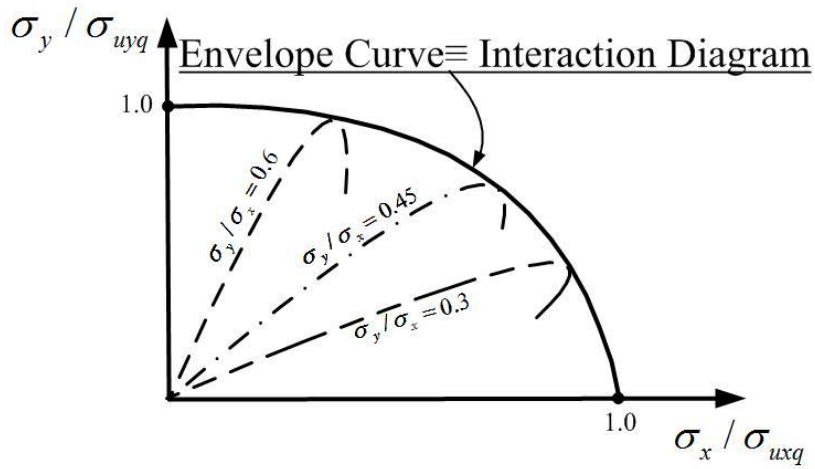


Figure 6: A typical interaction diagram.

Interaction diagrams for all models under different levels of lateral pressure have been shown in the Figures 7 to 9. Also, the collapse modes obtained for all stiffened models are represented in the Tables 3 to 5. Change of collapse modes from the simply-supported mode to the clamped mode is characterised in the results.

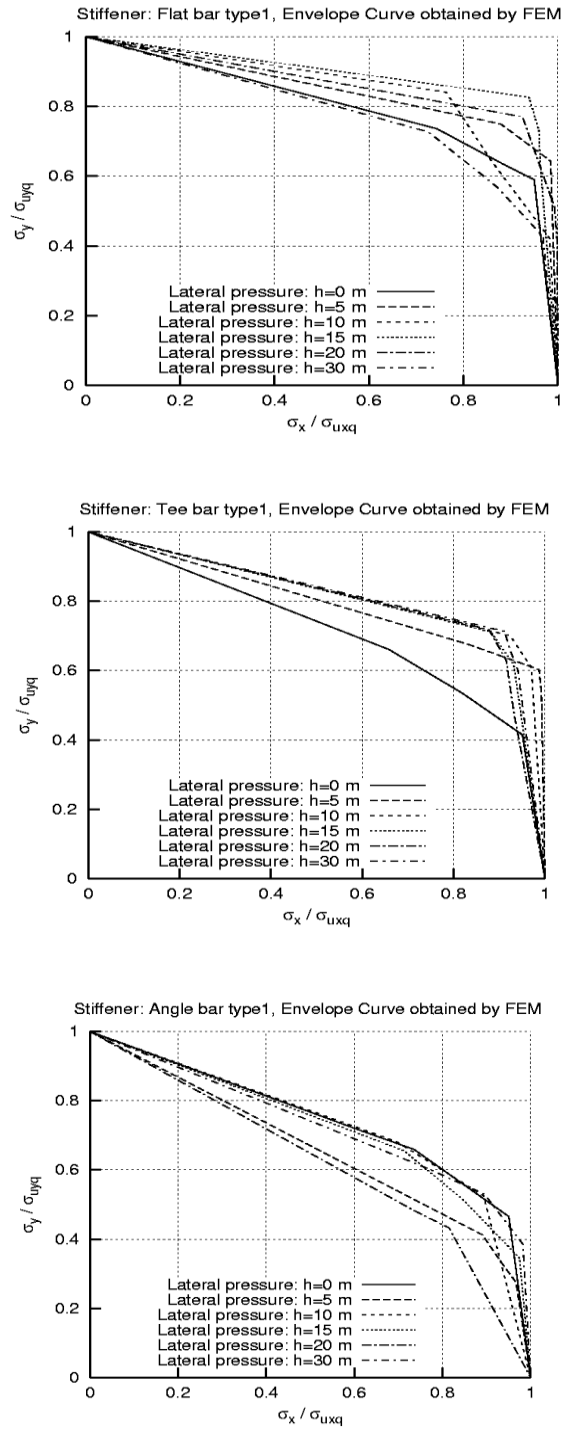
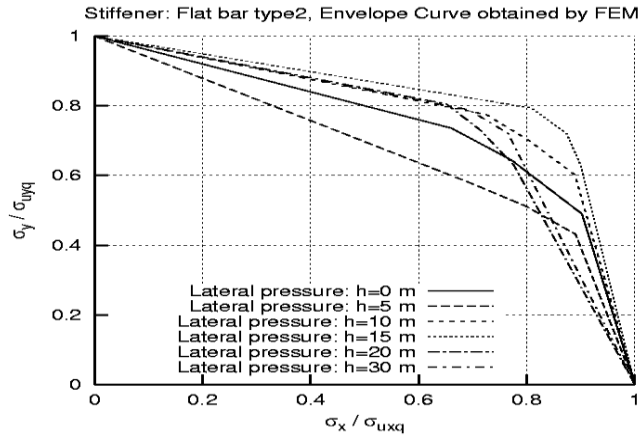
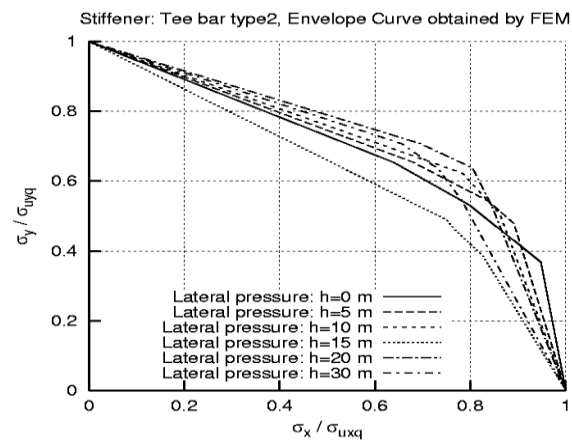


Figure 7: Interaction diagrams for the type 1 models (with L1, T1 and F1 Stiffeners).





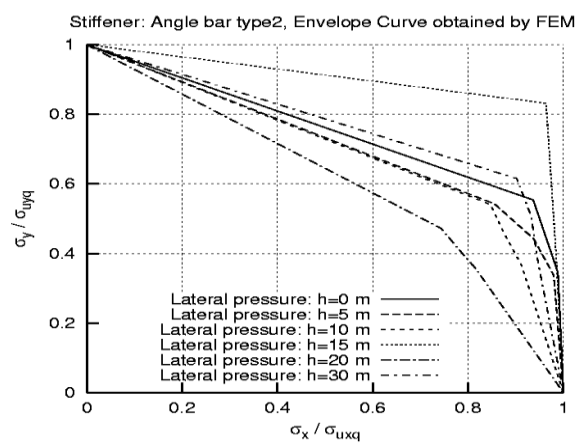


Figure 8: Interaction diagrams for the type 2 models (with L2, T2 and F2 Stiffeners).

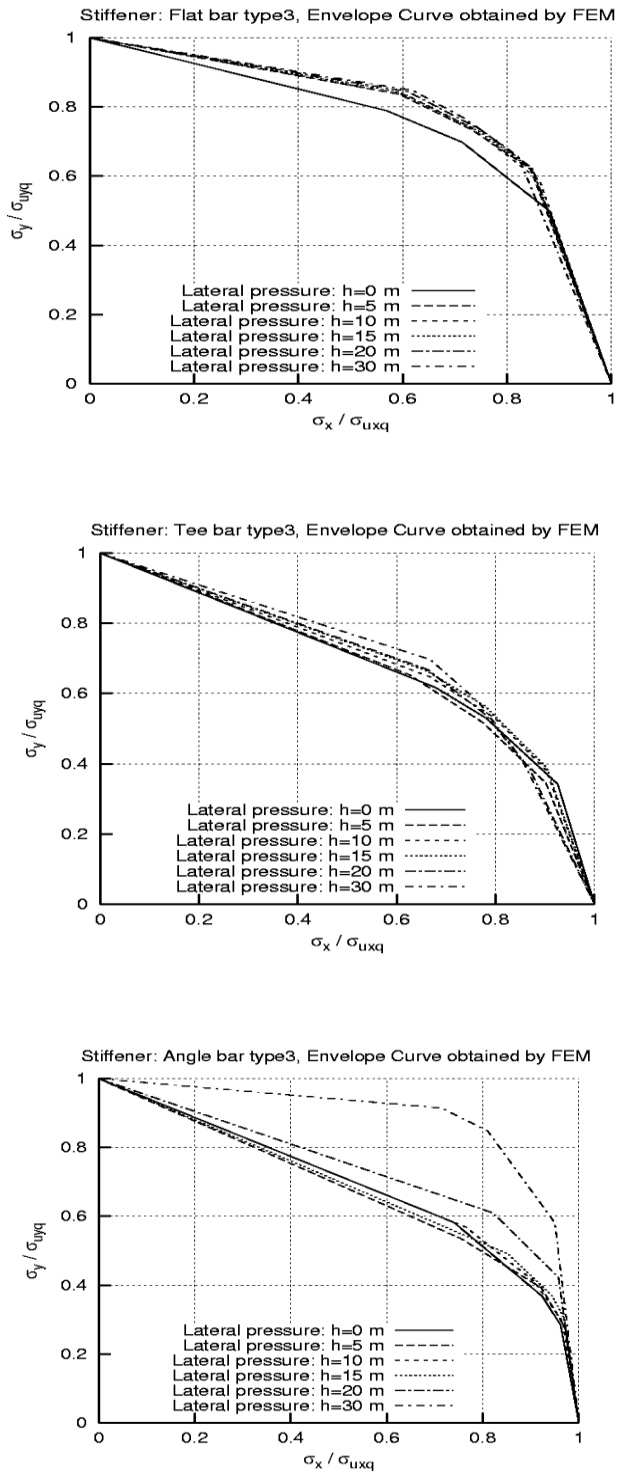


Figure 9: Interaction diagrams for the type 3 models (with L3, T3 and F3 Stiffeners).

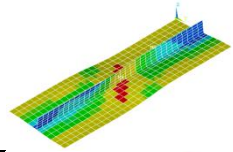
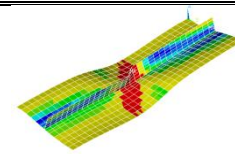
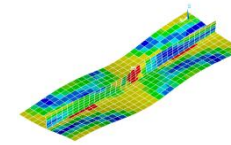
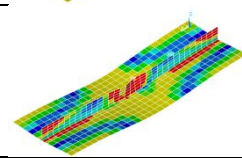
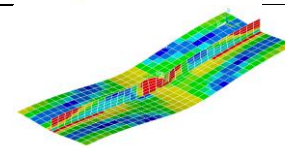
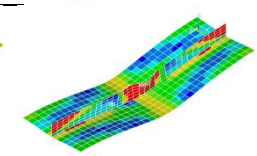
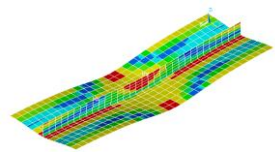
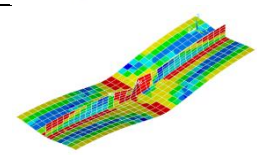
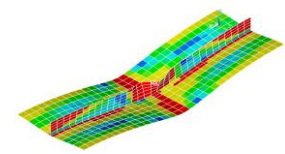
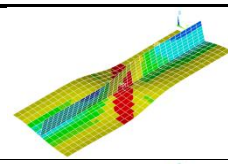
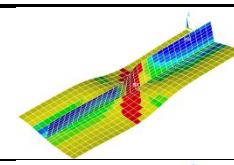
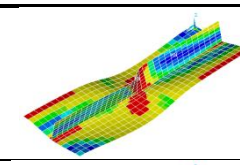
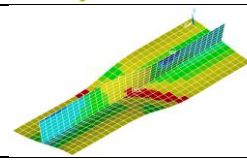
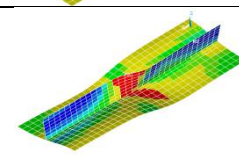
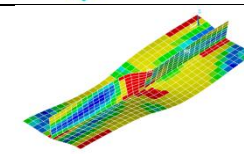
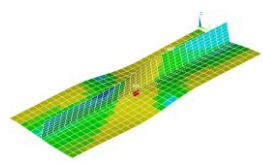
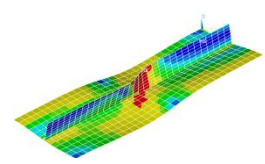
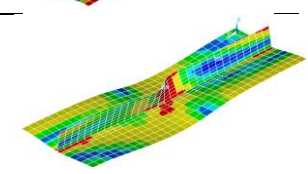
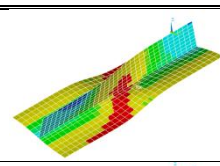
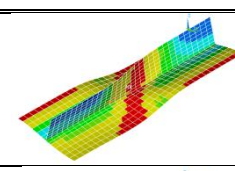
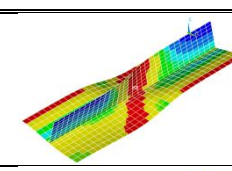
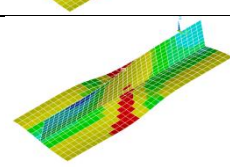
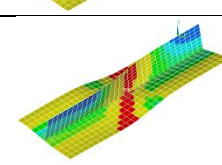
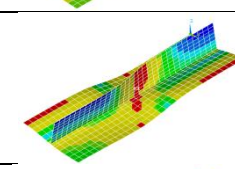
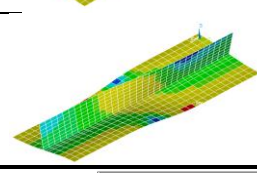
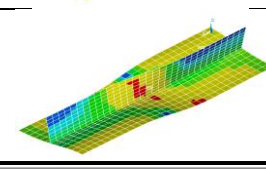
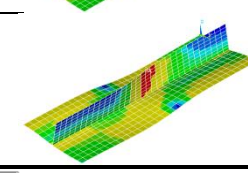
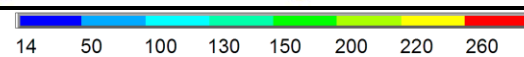
Type	$\sigma_Y : \sigma_X$	Lateral Water Pressure (h)		
		0 m	10 m	20 m
F1	0.6			
	0.45			
	0.3			
F2	0.6			
	0.45			
	0.3			
F3	0.6			
	0.45			
	0.3			
		 14 50 100 130 150 200 220 260 300		

Table 3: Collapse modes obtained using FEM for the stiffened aluminium plates having Flat-bar stiffeners.

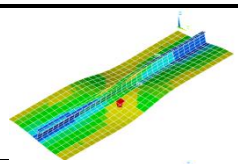
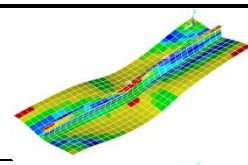
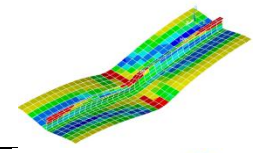
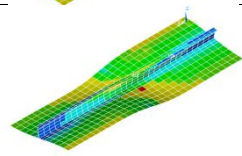
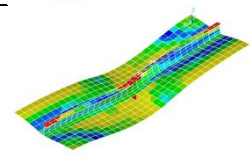
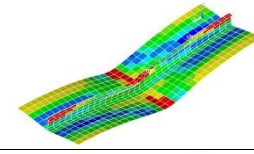
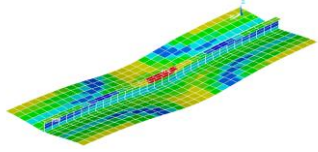
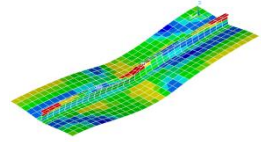
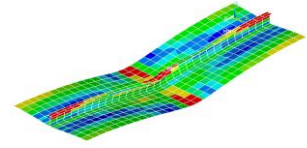
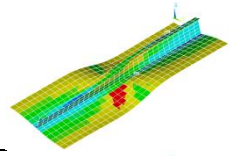
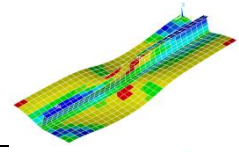
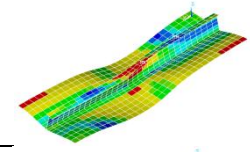
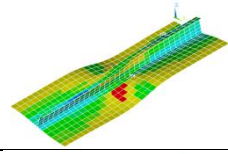
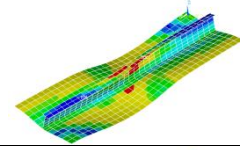
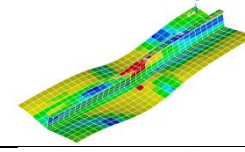
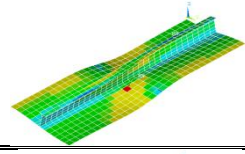
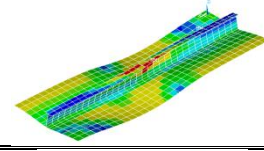
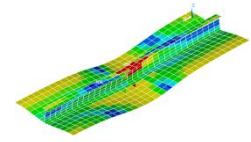
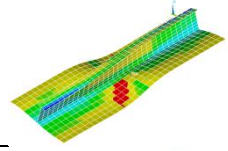
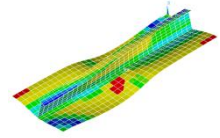
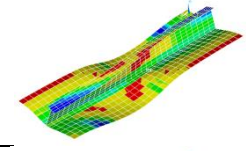
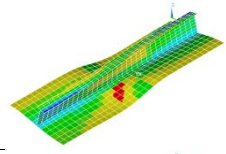
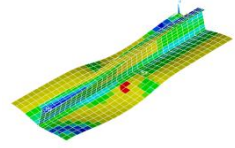
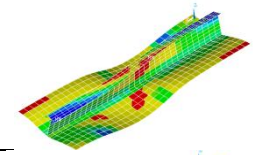
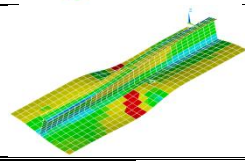
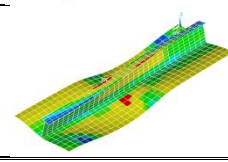
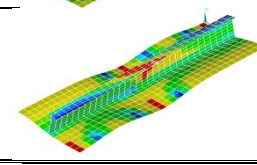
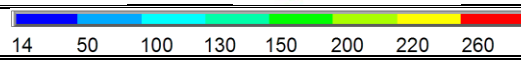
Type	$\sigma_Y : \sigma_X$	Lateral Water Pressure (h)		
		0 m	10 m	20 m
T1	0.6			
	0.45			
	0.3			
T2	0.6			
	0.45			
	0.3			
T3	0.6			
	0.45			
	0.3			
				

Table 4: Collapse modes obtained using FEM for the stiffened aluminium plates having Tee-bar stiffeners.

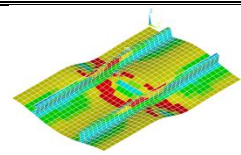
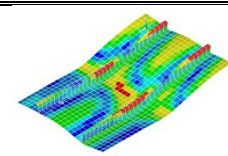
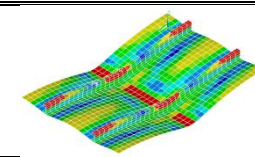
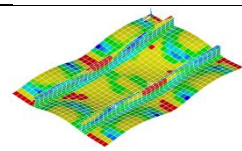
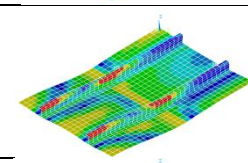
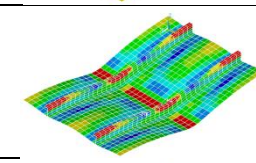
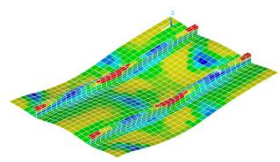
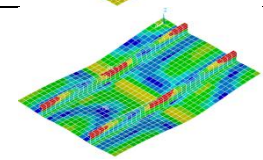
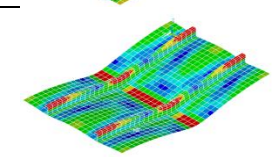
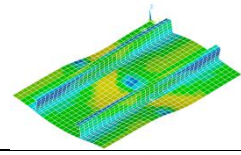
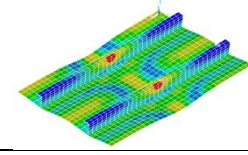
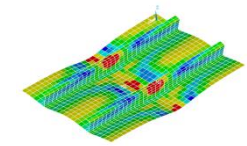
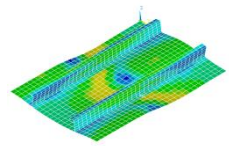
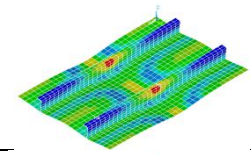
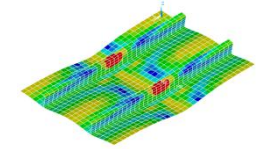
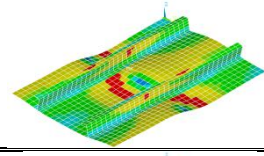
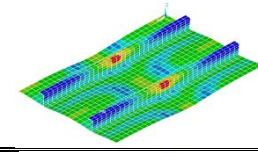
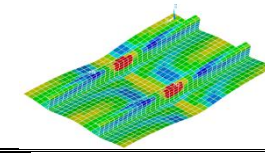
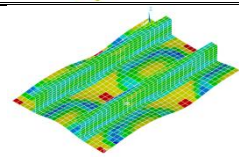
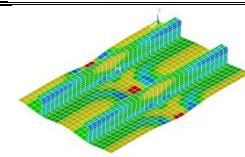
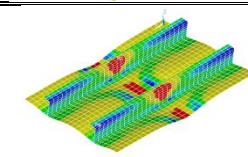
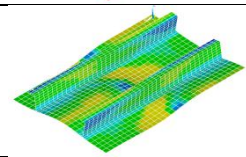
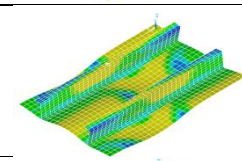
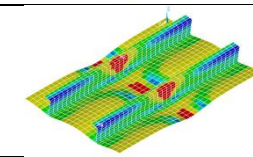
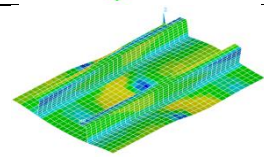
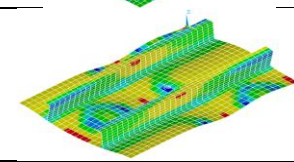
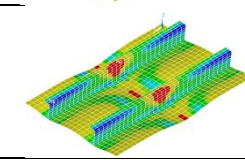
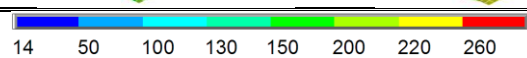
Type	$\sigma_Y : \sigma_X$	Lateral Water Pressure (h)		
		0 m	10 m	20 m
L1	0.6			
	0.45			
	0.3			
L2	0.6			
	0.45			
	0.3			
L3	0.6			
	0.45			
	0.3			
				

Table 5: Collapse modes obtained using FEM for the stiffened aluminium plates having Angle-bar stiffeners.

3 INTERACTION EQUATIONS

The following form or template is proposed for the interaction equation capable of predicting the ultimate strength of a continuous stiffened aluminium plate subject to combined biaxial compression and lateral pressure:

$$\left(\frac{\sigma_x}{\sigma_{uxq}}\right)^{a_1}+\left(\frac{\sigma_y}{\sigma_{uyq}}\right)^{a_2}=1 \tag{5}$$

where

$$\begin{aligned} a_1 &= c_1\beta + c_2\lambda + c_3 \\ a_2 &= d_1\beta + d_2\lambda + d_3 \end{aligned} \tag{6}$$

$$c_{1,2,3} = m_1 h^5 + m_2 h^4 + m_3 h^3 + m_4 h^2 + m_5 h + m_6$$

$$d_{1,2,3} = n_1 h^5 + n_2 h^4 + n_3 h^3 + n_4 h^2 + n_5 h + n_6$$

Performing the regression analysis on the previously-developed numerical database, different sets of the coefficients are derived.

3.1 Coefficients for the Case of Continuous Plates Stiffened with Flat-bar Stiffeners

The regression-based coefficients in this case would be as follows:

$$\begin{cases} c_1 = -0.0003064h^5 + 0.01943h^4 - 0.4059h^3 + 3.283h^2 - 9.412h + 0.623 \\ c_2 = 0.0008327h^5 - 0.05268h^4 + 1.087h^3 - 8.392h^2 + 21.22h - 2.524 \\ c_3 = 0.0004671h^5 - 0.02963h^4 + 0.6226h^3 - 5.146h^2 + 15.61h + 0.6036 \end{cases}$$
$$\begin{cases} d_1 = -0.0001402h^5 + 0.01094h^4 - 0.2972n_3h^3 + 3.227h^2 - 11.05h - 4.963 \\ d_2 = 0.000253h^5 - 0.02003h^4 + 0.5581h^3 - 6.317h^2 + 22.94h + 12.8 \\ d_3 = 0.0002563h^5 - 0.01987h^4 + 0.5348h^3 - 5.725h^2 + 19.24h + 10.44 \end{cases} \tag{7}$$

3.2 Coefficients for the Case of Continuous Plates Stiffened with Tee-bar Stiffeners

The regression-based coefficients in this case would be as follows:

$$\begin{cases} c_1 = 0.0000214h^5 - 0.001419h^4 + 0.03214h^3 - 0.2939h^2 + 0.8668h + 0.3475 \\ c_2 = -0.0002272h^5 + 0.01515h^4 - 0.3446h^3 + 3.154h^2 - 9.15h - 0.8782 \\ c_3 = 0 \end{cases}$$
$$\begin{cases} d_1 = -0.0000315h^5 + 0.002311h^4 - 0.06008h^3 + 0.6606h^2 - 2.614h + 0.6068 \\ d_2 = 0.0002977h^5 - 0.02186h^4 + 0.5689h^3 - 6.255h^2 + 24.5h + 3.262 \\ d_3 = 0 \end{cases} \tag{8}$$

3.3 Coefficients for the Case of Continuous Plates Stiffened with Angle-bar Stiffeners

The regression-based coefficients in this case would be as follows:

$$\begin{cases} c_1 = 0.0002218h^5 - 0.01432h^4 + 0.3053h^3 - 2.464h^2 + 6.241h + 0.6558 \\ c_2 = -0.0006212h^5 + 0.04009h^4 - 0.8545h^3 + 6.89h^2 - 17.34h - 1.918 \\ c_3 = 0 \end{cases} \quad (9)$$

$$\begin{cases} d_1 = 0.0000213h^5 - 0.001533h^4 + 0.03821h^3 - 0.3895h^2 + 1.381h + 0.4285 \\ d_2 = -0.0001589h^5 + 0.01123h^4 - 0.2742h^3 + 2.713h^2 - 9.535h + 5.308 \\ d_3 = 0 \end{cases}$$

4 VERIFICATION

The interaction equation (5) together with the powers (6) and coefficients (7) to (9) are now used to predict the ultimate strength of all models defined in Table 1 when subjected to different combinations of in-plane compression and lateral pressure. The numerical values of the ultimate strength for the analysed models are given in the Tables 6 to 8. In addition, comparison of the envelope curves predicted using the empirical interaction equations with those obtained using FEM for some typical cases is demonstrated in the Figure 10. As can be realised, a relatively good correlation can be observed among the results.

5 CONCLUSIONS

The aim of the present paper has been to develop closed form formulations for predicting ultimate compressive strength of stiffened aluminium plates under combined biaxial in-plane compression and lateral pressure. Extensive numerical results on welded stiffened aluminium plate structures obtained through a series of elastic-plastic large deflection FEM analyses were used for this purpose.

An easy-to-use and practical template is adopted for derivation of the empirical formulations for estimation of the ultimate strength in the form of interaction diagrams. Different constants and coefficients were derived in order to be implemented in that template for prediction of the ultimate strength of the plates stiffened with flat-bar/tee-bar/angle-bar stiffeners subject to various levels of water head. The ultimate strength formulations developed implicitly take into account the effects of weld-induced initial imperfections and softening in the heat affected zone. Accuracy of the derived formulations for the interaction diagrams was demonstrated through comparisons with the numerical results. The empirical formulations will be useful for ultimate strength-based reliability analyses of any aluminium plated structures. It should also be kept in mind that when using the derived empirical formulations for final sizing or detailed strength check calculations, any precautions are required such as additional safety factors given the potential for non-conservative strength predictions.

					Lateral Water Pressure (h)								
					0 m			10 m			20 m		
					FEM		Empirical Formula	FEM		Empirical Formula	FEM		Empirical Formula
Stiffener	Type	β	λ	$\frac{\sigma_Y}{\sigma_X}$	$\frac{\sigma_X}{\sigma_{uxq}}$	$\frac{\sigma_Y}{\sigma_{uyq}}$	$\frac{\sigma_Y}{\sigma_{uyq}}$	$\frac{\sigma_X}{\sigma_{uxq}}$	$\frac{\sigma_Y}{\sigma_{uyq}}$	$\frac{\sigma_Y}{\sigma_{uyq}}$	$\frac{\sigma_X}{\sigma_{uxq}}$	$\frac{\sigma_Y}{\sigma_{uyq}}$	$\frac{\sigma_Y}{\sigma_{uyq}}$
F bar	F1	2.603	0.787	1.0:0.0	0	1	1	0	1	1	0	1	1
				0.60	0.743	0.736	0.454	0.762	0.841	0.855	0.924	0.769	0.844
				0.45	0.879	0.637	0.202	0.859	0.642	0.673	0.992	0.510	0.620
				0.30	0.949	0.589	0.071	0.975	0.589	0.574	0.998	0.408	0.497
				0.0:1.0	1	0	0	1	0	0	1	0	0
	F2	2.603	0.426	1.0:0.0	0	1	1	0	1	1	0	1	1
				0.60	0.660	0.735	0.721	0.725	0.774	0.777	0.651	0.804	0.948
				0.45	0.772	0.643	0.633	0.805	0.698	0.709	0.715	0.728	0.913
				0.30	0.902	0.489	0.478	0.889	0.601	0.608	0.776	0.629	0.864
				0.0:1.0	1	0	0	1	0	0	1	0	0
	F3	2.278	0.273	1.0:0.0	0	1	1	0	1	1	0	1	1
				0.60	0.569	0.789	0.784	0.607	0.833	0.839	0.610	0.843	0.946
				0.45	0.714	0.697	0.679	0.732	0.738	0.747	0.749	0.733	0.879
				0.30	0.881	0.497	0.491	0.862	0.587	0.598	0.848	0.621	0.789
				0.0:1.0	1	0	0	1	0	0	1	0	0

Table 6: Comparison of the ultimate strength values predicted using the empirical interaction equations with those obtained using FEM for the stiffened aluminium plates having Flat-bar stiffeners.

					Lateral Water Pressure (h)								
					0 m			10 m			20 m		
						FEM	Empirical Formula		FEM	Empirical Formula		FEM	Empirical Formula
Stiffener	Type	β	λ	$\frac{\sigma_Y}{\sigma_X}$	$\frac{\sigma_X}{\sigma_{uxq}}$	$\frac{\sigma_Y}{\sigma_{uyq}}$	$\frac{\sigma_Y}{\sigma_{uyq}}$	$\frac{\sigma_X}{\sigma_{uxq}}$	$\frac{\sigma_Y}{\sigma_{uyq}}$	$\frac{\sigma_Y}{\sigma_{uyq}}$	$\frac{\sigma_X}{\sigma_{uxq}}$	$\frac{\sigma_Y}{\sigma_{uyq}}$	$\frac{\sigma_Y}{\sigma_{uyq}}$
T bar	T1	3.037	0.790	1.0:0.0	0	1	1	0	1	1	0	1	1
				0.60	0.658	0.660	0.0.641	0.845	0.751	0.742	0.877	0.717	0.638
				0.45	0.819	0.534	0.546	0.923	0.700	0.718	0.914	0.630	0.472
				0.30	0.950	0.414	0.404	0.970	0.609	0.563	0.933	0.469	0.375
				0.0:1.0	1	0	0	1	0	0.032	1	0	0
	T2	3.037	0.411	1.0:0.0	0	1	1	0	1	1	0	1	1
				0.60	0.639	0.653	0.660	0.783	0.622	0.682	0.694	0.707	0.787
				0.45	0.796	0.532	0.546	0.861	0.506	0.577	0.804	0.638	0.648
				0.30	0.947	0.368	0.353	0.945	0.411	0.401	0.844	0.530	0.580
				0.0:1.0	1	0	0	1	0	0	1	0	0
	T3	3.037	0.271	1.0:0.0	0	1	1	0	1	1	0	1	1
				0.60	0.679	0.616	0.619	0.665	0.648	0.596	0.661	0.668	0.455
				0.45	0.781	0.529	0.536	0.797	0.530	0.465	0.778	0.540	0.363
				0.30	0.925	0.341	0.359	0.902	0.380	0.324	0.868	0.386	0.277
				0.0:1.0	1	0	0	1	0	0	1	0	0

Table 7: Comparison of the ultimate strength values predicted using the empirical interaction equations with those obtained using FEM for the stiffened aluminium plates having Tee-bar stiffeners.

					Lateral Water Pressure (h)								
					0 m			10 m			20 m		
						FEM	Empirical Formula		FEM	Empirical Formula		FEM	Empirical Formula
Stiffener	Type	β	λ	$\frac{\sigma_Y}{\sigma_X}$	$\frac{\sigma_X}{\sigma_{uxq}}$	$\frac{\sigma_Y}{\sigma_{uyq}}$	$\frac{\sigma_Y}{\sigma_{uyq}}$	$\frac{\sigma_X}{\sigma_{uxq}}$	$\frac{\sigma_Y}{\sigma_{uyq}}$	$\frac{\sigma_Y}{\sigma_{uyq}}$	$\frac{\sigma_X}{\sigma_{uxq}}$	$\frac{\sigma_Y}{\sigma_{uyq}}$	$\frac{\sigma_Y}{\sigma_{uyq}}$
L bar	L1	3.037	0.790	1.0:0.0	0	1	1	0	1	1	0	1	1
				0.60	0.613	0.714	0.751	0.696	0.681	0.764	0.733	0.483	0.453
				0.45	0.735	0.574	0.695	0.893	0.525	0.582	0.814	0.421	0.412
				0.30	0.950	0.465	0.506	0.972	0.465	0.421	0.925	0.351	0.362
				0.0:1.0	1	0	0	1	0	0	1	0	0
	L2	3.037	0.411	1.0:0.0	0	1	1	0	1	1	0	1	1
				0.60	0.887	0.621	0.602	0.846	0.540	0.597	0.743	0.471	0.362
				0.45	0.936	0.553	0.476	0.873	0.463	0.555	0.778	0.414	0.314
				0.30	0.988	0.344	0.292	0.911	0.366	0.483	0.815	0.356	0.267
				0.0:1.0	1	0	0	1	0	0	1	0	0
	L3	3.037	0.271	1.0:0.0	0	1	1	0	1	1	0	1	1
				0.60	0.739	0.582	0.687	0.765	0.567	0.671	0.742	0.682	0.645
				0.45	0.923	0.368	0.448	0.907	0.409	0.436	0.821	0.609	0.510
				0.30	0.961	0.284	0.348	0.966	0.292	0.264	0.957	0.421	0.227
				0.0:1.0	1	0	0	1	0	0	1	0	0

Table 8: Comparison of the ultimate strength values predicted using the empirical interaction equations with those obtained using FEM for the stiffened aluminium plates having Angle-bar stiffeners.

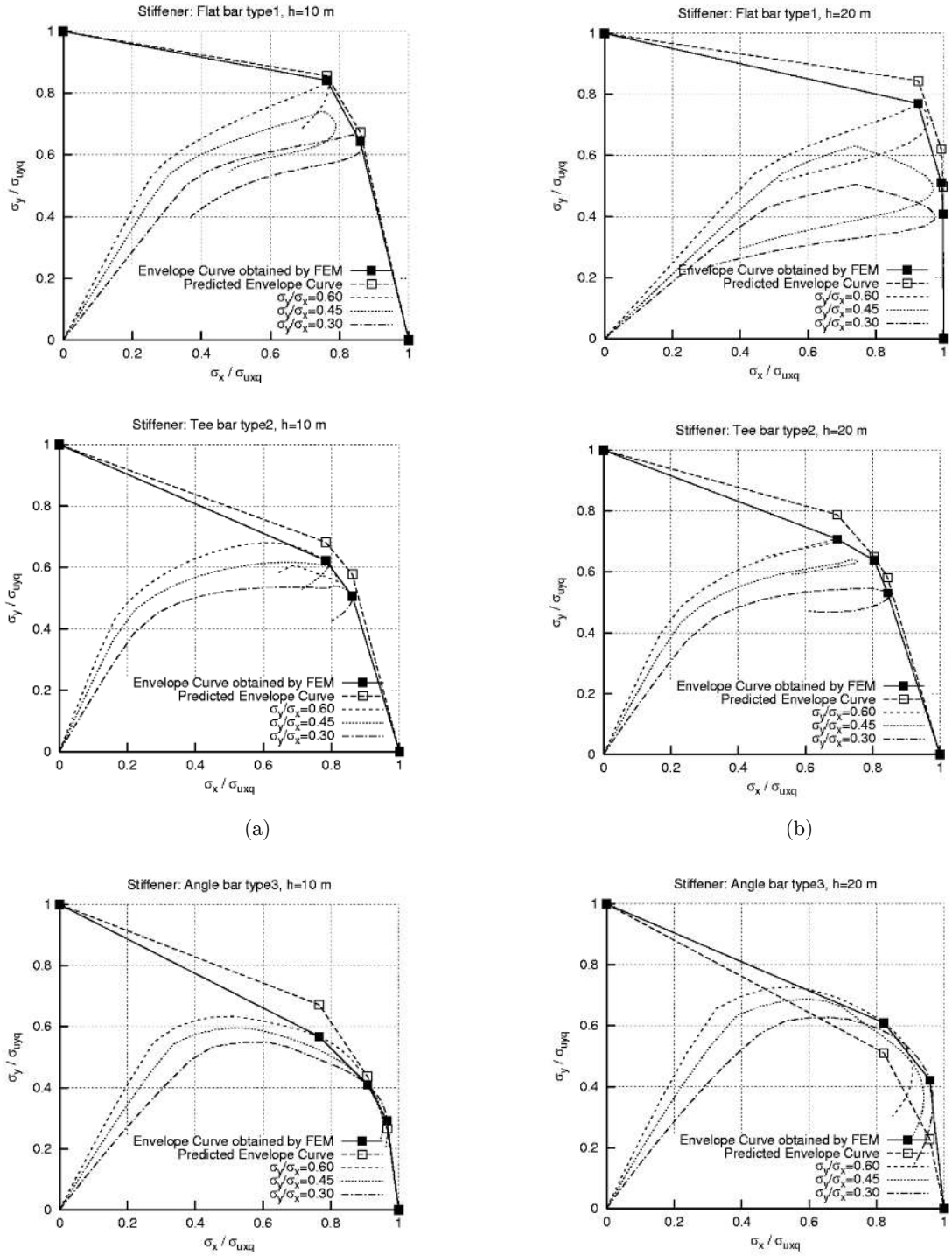


Figure 10: Comparison of the envelope curves predicted using the empirical interaction equations with those obtained using FEM for some typical cases.

References

Aalberg, A., Langseth, M., Malo, K.A., (1998). Ultimate strength of stiffened aluminium plates, Norwegian University of Science and Technology, Department of Structural Engineering.

ANSYS User's Manual (Version 7.1), Houston, Swanson Analysis Systems Inc. (2003).

Hopperstad, O.S., Langseth, M., Hanssen, L., (1998). Ultimate compressive strength of plate elements in aluminium: correlation of finite element analyses and tests, Thin-Walled Struct. 29: 31–46.

Khedmati, M.R., (2000). Ultimate strength of ship structural members and systems considering local pressure loads, Dr. Eng. Thesis, Graduate School of Engineering, Hiroshima University.

Khedmati, M.R., Bayatfar, A., Rigo, P., (2010*a*). Post-buckling behaviour and strength of multi-stiffened aluminium panels under combined axial compression and lateral pressure, Marine Struct. 23(1): 39-66.

Khedmati, M.R., Memarian, H.R., Fadavie, M., Zareei, M.R., (2014*a*). Elastic-Plastic Large Deflection Analysis of Continuous Stiffened Aluminium Plates under Combined Transverse In-plane Compression and Lateral Pressure, Sadhana - Academy Proceedings in Engineering Science. (under review).

Khedmati, M.R., Memarian, H.R., Fadavie, M., Zareei, M.R., (2014*b*). Empirical formulations for estimation of ultimate strength of continuous stiffened aluminium plates under combined transverse in-plane compression and lateral pressure, Ships and Offshore Struct. (under review).

Khedmati, M.R., Zareei, M.R., Rigo, P., (2009). Sensitivity analysis on the elastic buckling and ultimate strength of continuous stiffened aluminium plates under combined in-plane compression and lateral pressure, Thin-Walled Struct. 47(11): 1232-1245.

Khedmati, M.R., Zareei, M.R., Rigo, P., (2010*b*). Empirical formulations for estimation of ultimate strength of continuous stiffened aluminium plates under combined in-plane compression and lateral pressure, Thin-Walled Struct. 48(3):274-289.

Memarian, H.R., (2011). Buckling/ultimate strength analysis of stiffened aluminium plates subjected to combined biaxial compression and lateral pressure, MSc Thesis, Department of Marine Technology, Amirkabir University of Technology.

Paik, J.K., (2007). Empirical formulations for predicting the ultimate compressive strength of welded aluminum stiffened panels, Thin-Walled Struct. 45:171-184.

Paik, J.K., Andrieu, C., Cojeen, H.P., (2008). Mechanical collapse testing on aluminium stiffened plate structures for marine applications, Marine Technology 45(4): 228-240.

Paik, J.K., Hughes, O.F., Hess, P.E., Renaud, C., (2005). Ultimate limit state design technology for aluminium multi-hull ship structures, Trans. SNAME 113: 270-305.

Paik, J.K., Thayamballi, A.K., Ryu, J.Y., Jang, J.H., Seo, J.K., Park, S.W., Seo, S.K., Renayd, C., Cojeen, H.P., Kim, N.I., (2006). The statistics of weld induced initial imperfections in aluminium stiffened plate structures for marine applications, International Journal of Maritime Engineering 148(4):19-63.

Rigo, P., Sarghiuta, R., Estefen, S., Lehmann, E., Otelea, S.C., Pasqualino, I., Simonsen, B.C., Wan, Z. Yao, T. (2003). Sensitivity analysis on ultimate strength of aluminium stiffened panels, Marine Struct. 16: 437–468.

Smith, C.S., Davidson, P.C., Chapman, J.C., Dowling, P.J., (1987). Strength and stiffness of ships' plating under in-plane compression and tension, Trans. RINA 129: 277-296.

Varghese, B., (1998). Buckling/plastic collapse strength of plates and stiffened plates under combined loads, Dr. Eng. Thesis, Hiroshima University.

Yao, T., Fujikubo, M., Yanagihara, D., Irisawa, M., (1998). Consideration on FEM modelling for buckling/plastic collapse analysis of stiffened plates, Trans. of the West-Japan Soc. Naval Arch. 85: 121-128 (in Japanese).

Zha, Y., Moan, T., (2003). Experimental and numerical prediction of collapse of flat-bar stiffeners in aluminium panels, J. Struct. Eng. 129(2): 160–8.

Zha, Y., Moan, T., Hanken, E., (2001). Ultimate strength of stiffened aluminium panels with predominantly tensional failure modes, Thin-Walled Struct. 39: 631–48.